

NEUTRINO OSCILLATION EXPERIMENTS

CALT--63-495

F. Boehm

DE89 010027

California Institute of Technology, Pasadena, Ca 91125

Abstract

We review the status and results of neutrino oscillation experiments with emphasis on non-accelerator experiments. To date there is no confirmed evidence for neutrino oscillations, with limits for the mass parameter Δm^2 of 2×10^{-2} eV² for full mixing, and limits for mixing angles $\sin^2 2\theta$ of about 10^{-3} for large Δm^2 .

Introduction

If evidence were found that neutrinos have mass, this would constitute a clear signal for new physics beyond the Standard Model. One of the manifestations of neutrino mass is the phenomenon of neutrino oscillations, i.e. transition from one neutrino flavor into another one (see, e.g. ref. 1). For oscillations to occur, neutrinos, in addition to having mass, must be mixed states, in the sense that the weak interaction neutrino states ν_l are superpositions of mass eigenstates ν_i ,

$$\nu_l = \sum_i U_{l,i} \nu_i, \quad l = e, \mu, \tau.$$

MASTER

The results of oscillation experiments are usually given in terms of a two-parameter model for neutrino oscillations characterized by the mass parameter

DISTRIBUTION OF THIS DOCUMENT IS UNLIMITED

Invited talk at the Rochester Workshop on Non-Accelerator Particle Physics,
Rochester, New York, June 1987.

DISCLAIMER

This report was prepared as an account of work sponsored by an agency of the United States Government. Neither the United States Government nor any agency thereof, nor any of their employees, makes any warranty, express or implied, or assumes any legal liability or responsibility for the accuracy, completeness, or usefulness of any information, apparatus, product, or process disclosed, or represents that its use would not infringe privately owned rights. Reference herein to any specific commercial product, process, or service by trade name, trademark, manufacturer, or otherwise does not necessarily constitute or imply its endorsement, recommendation, or favoring by the United States Government or any agency thereof. The views and opinions of authors expressed herein do not necessarily state or reflect those of the United States Government or any agency thereof.

DISCLAIMER

Portions of this document may be illegible in electronic image products. Images are produced from the best available original document.

$\Delta m^2 = |m_2^2 - m_1^2|$ and the mixing strength $\sin^2 2\theta$.

In the spirit of this Conference on Non-Accelerator Particle Physics I shall focus here on reactor based oscillation experiments. Nuclear power reactors are prolific sources for $\bar{\nu}_e$ having source strengths of about 5×10^{20} per second, with a neutrino energy up to about 10 MeV. If there are neutrino oscillations, the neutrinos $\bar{\nu}_e$ will disappear with a probability,

$$P_{\bar{\nu}_e} = 1 - \sin^2 2\theta \sin^2 1.27 \frac{\Delta m^2 (eV^2) L (m)}{E_\nu (MeV)}$$

where L is the distance in m between neutrino source and detector, and E_ν is the neutrino energy in MeV . For a given Δm^2 , the sensitivity of an experiment depends on L/E_ν . Figure 1 illustrates the regions of L/E_ν for reactor experiments in comparison to other oscillation experiments.

Results of Reactor Experiments

A summary of reactor experiments is shown in Table 1, giving the distance between core and detector, the number of events, and a brief characterization of the detector. In the following I shall describe a series of experiments performed by the Caltech-SIN-TU Munich collaboration³ at the Gösgen power reactor in Switzerland. Three experiments have been carried out between 1981 and 1985 with the detector at distances of 37.8m, 45.9m, and 64.7m from the reactor core (henceforth denoted as experiments I, II, and III).

The detector consisted of an array of liquid scintillation counters and ${}^3\text{He}$ multiwire proportional chambers, surrounded by an active scintillation veto counter and various shieldings, as illustrated in Figures 2 and 3. The detector is based in the reaction $\bar{\nu}_e + p = e^+ + n$. The signature of an event is given by a positron pulse in the liquid scintillator followed by a neutron induced reaction in the ${}^3\text{He}$ counter. The time correlation and time window chosen are shown in Figure 4. Pulse shape discrimination (PSD) helped greatly to reduce background events associated with fast neutrons from cosmic rays, as illustrated in Figure 5. No reactor associated background was seen, as could be verified by comparing backgrounds with reactor-on and reactor-off (see Figure 5).

The observed correlated positron spectrum was corrected for the detector response as a function of energy and position. Both corrections were studied with test sources as well as with Monte Carlo simulations, taking into account the neutrino interaction in the scintillation liquid and in the Lucite walls of the detector cells. Positron finite range, annihilation at rest and in flight, as well as bremsstrahlung were taken into account. The final experimental spectra are shown in Figure 6.

In order to compare spectra at various positions, the relative reactor spectrum for each experiment had to be known. Small differences in reactor fuel composition were taken into account, although these differences were minimized by conducting each experiment over a full fuel cycle. Figure 7 shows the fuel composition of the Gossigen core as a function of time, together with the actual experimental cycles for each experiment. From the relative differences of fuel composition, the relative spectra shown in Figure 8 were derived. As can be seen, the differences in the spectra amount

to less than about 5% with a negligibly small uncertainty. In the data analysis the experimental positron spectra were compared to calculated spectra given by an expression (see Ref. 3) that contains the product of the detector efficiency, a coefficient that accounts for the small difference in fuel composition, the cross section, the neutrino spectrum $S(E_\nu)$ and the oscillation function $P(E_\nu, L, \Delta m^2, \theta)$, all this integrated over the energy resolution function of the detector and the finite solid angle.

The data were analyzed in two different ways, as briefly outlined below:

An first analysis (Analysis A) independent of the source neutrino spectrum was conducted. The neutrino spectrum $S(E_\nu)$ is parametrized as:

$$S_A(E_\nu) = e^{(A_0 + A_1 E + A_2 E^2)}$$

and a χ^2 is calculated for the difference between the experimental yield and the expected yield obtained in the manner described above, summed over all the data bins and positions. The χ^2 was minimized for a fixed set of parameters Δm^2 and $\sin^2 2\theta$ by varying the coefficients A_0 , A_1 , and A_2 and three normalization coefficients, one for each position. For no-oscillations it was found that $\chi^2(0,0) = 41.1/45$. A maximum likelihood test was used to obtain the exclusion plot shown in Figure 9. There is no evidence for oscillations and the parameter region excluded at 90% c.l. is to the right of the curves. The expected positron spectra from this analysis (solid lines) are also shown in Figure 6.

Analysis B is based on neutrino spectra $S_\beta(E_\nu)$ obtained from measured on-line electron spectra of the fission targets ^{235}U and ^{239}Pu and from calculated spectra for

fission of ^{238}U and ^{241}Pu . These spectra are also shown in Figure 6 (dashed lines) and agree quite well with the experimental spectra. All three spectra are displayed as a function of L/E_ν in Figure 10. Exclusion plots obtained by similar procedures are shown in Figure 11.

The recent experiments at Savannah River have now also provided data at two positions⁵. The detector, a Gd loaded liquid scintillation counter detected both the positrons and the neutrons. We indicate in Figure 9 the excluded region obtained in these experiments.

Another recent experiment by Afonin et al.⁶ at the Rovno power reactor near Moscow measures the integral neutrino yield. For comparison we have drawn the exclusion plots obtained for a single position (18.5 m) and for two positions (18.5 m and 25m) in Figures 9 and 11, respectively.

The exclusion plots in Figure 9 also include the work at the Bugey reactor published three years ago by Cavaignac et al.⁴ The Bugey results are indicative for oscillations with allowed parameters within the shaded area, and with a most likely value of ($\Delta^2 = 0.2 \text{ eV}^2$, $\sin^2 2\theta = 0.25$). These results do not agree at a high confidence level with the Gösgen data, and the disagreement is presently not understood.

Conclusion

Results for the integral ratios of the experimental spectra at various positions are shown in Table II. These ratios are consistent with 1.0 (no oscillations) except for the Bugey data.

For completeness, Figure 12 gives a summary of the excluded regions in recent high energy accelerator experiments. Tentative evidence for oscillations in PS191 (ref. 10) is not confirmed by several other experiments.

To summarize the present status of oscillation experiments, we show in Figure 13 the result of high energy experiments and reactor experiments, as well as the expected area in the parameter space from the solar neutrino flux from ${}^8\text{B}$ interpreted in terms of matter oscillations ¹.

What are the sensitivities that might be reached in the near future in reactor experiments? The present limits for Δm^2 for full mixing of $\Delta m^2 < 0.02 \text{ eV}^2$ (90 c.l.) and of $\sin^2 2\theta > 0.2$ for large Δm^2 might be improved somewhat, but probably not more than a factor of two.

While the experiments at Gosgen are now completed, several other oscillation searches listed in Table I are still ongoing. In particular, Bugey plans to install three detectors at three different positions. Data taking at Savannah River and Rovno will continue and in each case might be supplemented by data from a new, third position. This should help to shed light on the discrepancy with the Bugey data.

To substantially improve the sensitivity of Δm^2 , say by a factor of 10, one needs to enlarge by a factor of 10 the distance between source and detector, from the present 65m to 650m. Figure 14 illustrates the situation for a hypothetical detector at 650 m. In order to obtain comparable statistical accuracy, this detector must be 100 times larger in target volume compared to the present Gosgen detector, and, in addition, should possess a higher efficiency to compensate for the lower signal-to-noise ratio. To build such a 40 ton liquid scintillation detector is clearly a major undertaking.

It may be justified on its own merits, although one should keep in mind that its maximum sensitivity of $\Delta m^2 < 0.002 \text{ eV}^2$ is still one or two orders of magnitude away from the Δm^2 region where possible effects from matter oscillations might be expected.

DISCLAIMER

This report was prepared as an account of work sponsored by an agency of the United States Government. Neither the United States Government nor any agency thereof, nor any of their employees, makes any warranty, express or implied, or assumes any legal liability or responsibility for the accuracy, completeness, or usefulness of any information, apparatus, product, or process disclosed, or represents that its use would not infringe privately owned rights. Reference herein to any specific commercial product, process, or service by trade name, trademark, manufacturer, or otherwise does not necessarily constitute or imply its endorsement, recommendation, or favoring by the United States Government or any agency thereof. The views and opinions of authors expressed herein do not necessarily state or reflect those of the United States Government or any agency thereof.

Figure Captions

- Fig. 1 Illustration of the region of L/E_ν accessible for various experiments.
- Fig. 2 Neutrino detector at Gosgen. The central neutrino detector unit consists of 30 liquid scintillator cells, arranged in five planes, for positron detection, and four ^3He filled wire chambers for neutron detection.
- Fig. 3 Detector assembly for the neutrino experiment at Gosgen. (1) Central Detector, (2) Veto house, (4) Water shield (5) Lead shield.
- Fig. 4 Distribution of time intervals between neutrino induced events in a scintillator cell and a wire chamber. The shaded area corresponds to the employed time window of $250 \mu\text{s}$.
- Fig. 5 Example of a PSD spectrum obtained in experiment II for reactor-on data (solid line) and reactor-off data (dashed line). The channel number is proportional to the decay time of the light pulse associated with the recoiling particle. For reactor-on data the peak on the left is enhanced due to neutrino induced positrons, while the neutron peak on the right remains unchanged.
- Fig. 6 Measured and predicted positron yields for experiments I to III. The solid lines represent the predicted positron yields derived by using the data from experiments I to III (Analysis A). The dashed lines represent the predicted positron yields derived by using the spectrum based on independent β -spectroscopic data. (Analysis B).

- Fig. 7 Relative contributions to the number of fissions from the four relevant isotopes as a function of days of reactor at full power. The data taking periods of experiments I to III are indicated.
- Fig. 8 Relative changes of the reactor antineutrino yields of experiments II and III, as compared to the yield of experiment I, as a function of the neutrino energy. These differences are caused by slight changes in the reactor fuel compositions for the individual measuring periods.
- Fig. 9 Exclusion plots for oscillation parameters Δm^2 and $\sin^2 2\theta$ from 3-position experiments at Gosgen, 2-position experiments at Bugey, Rovno, and Savanhah River. In the Bugey experiment the shaded area is allowed, in all other experiments the area to the right of the curve is forbidden. The Rovno results are based on the integral yield only.
- Fig. 10 Display of positron spectra from the ILL experiments and the three Goëgen experiments vs L/E_ν . The positron yield divided by the expected yield for no oscillation is plotted.
- Fig. 11 Exclusion plots based on predicted neutrino spectrum (Gosgen) and predicted integral yield (Rovno).
- Fig. 12 Limits from high energy experiments. BEBC: ref. 7, CHARM: ref. 8, BNL: ref. 9, PS191: ref. 10, LANL: ref. 11.
- Fig. 13 Limits for neutrino oscillations from various experiments. The dotted curve below the Gosgen line is for a hypothetical experiment at 650 m.
- Fig. 14 Illustration of the Gosgen data and some hypothetical data with a detector of 650 m. Curves show the expected yields for full mixing and $\Delta m^2 = 0.02 \text{ eV}^2$, and $\Delta m^2 = 0.002 \text{ eV}^2$.

References

- [1] F. Boehm and P. Vogel, *Physics of Massive Neutrinos*, Cambridge University Press, Cambridge, 1987.
- [2] H. Kwon et al., Phys. Rev. D24, 1097 (1981).
- [3] G. Zacek et at., Phys. Rev. D34, 2621 (1986).
- [4] J.-F. Cavaignac et al., Phys. Lett. B148, 387 (1984).
- [5] H. Sobel, in *Neutrino 86, Proc. 12th Int. Conf. Neutrino Physics and Astrophysics*, Sendai, p. 148, eds. T. Kitagaki and H. Yuta. Singapore, World Scientific, 1986.
- [6] A. Afonin et al., JETP Lett. 42, 285 (1985).
- [7] C. Angelini et al., Phys. Lett. B179, 307 (1986)
- [8] F. Bergsma et al., Phys. Lett. B142, 103 (1984).
- [9] T. Ahrens et al., Phys. Rev. D31, 2732 (1985).
- [10] G. Bernardi et al., Phys. Lett. B181, 173 (1986).
- [11] T. Dombeck et al., LANL preprint, 1987.

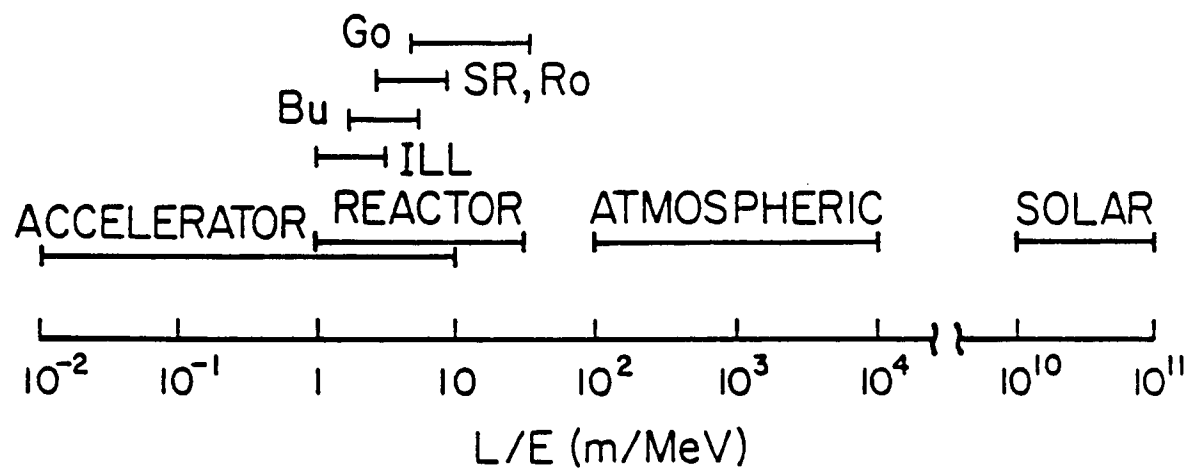
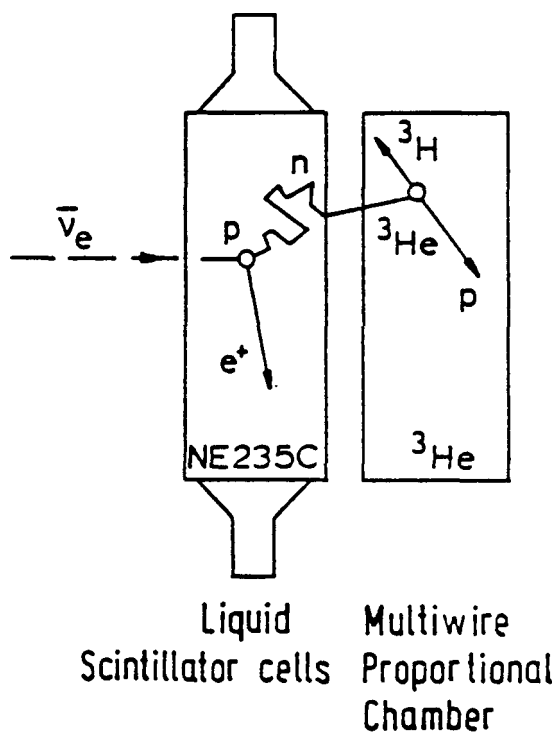


Fig. 1

Detection principle



Detector assembly

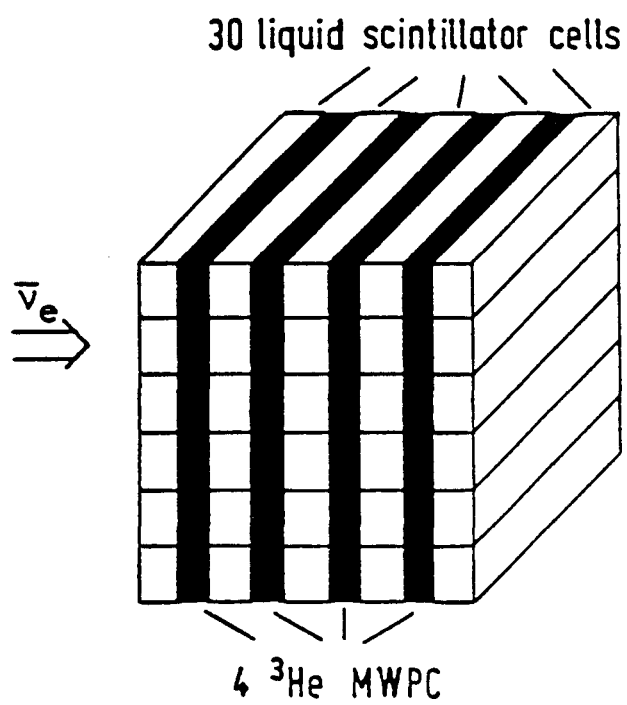


Fig. 2

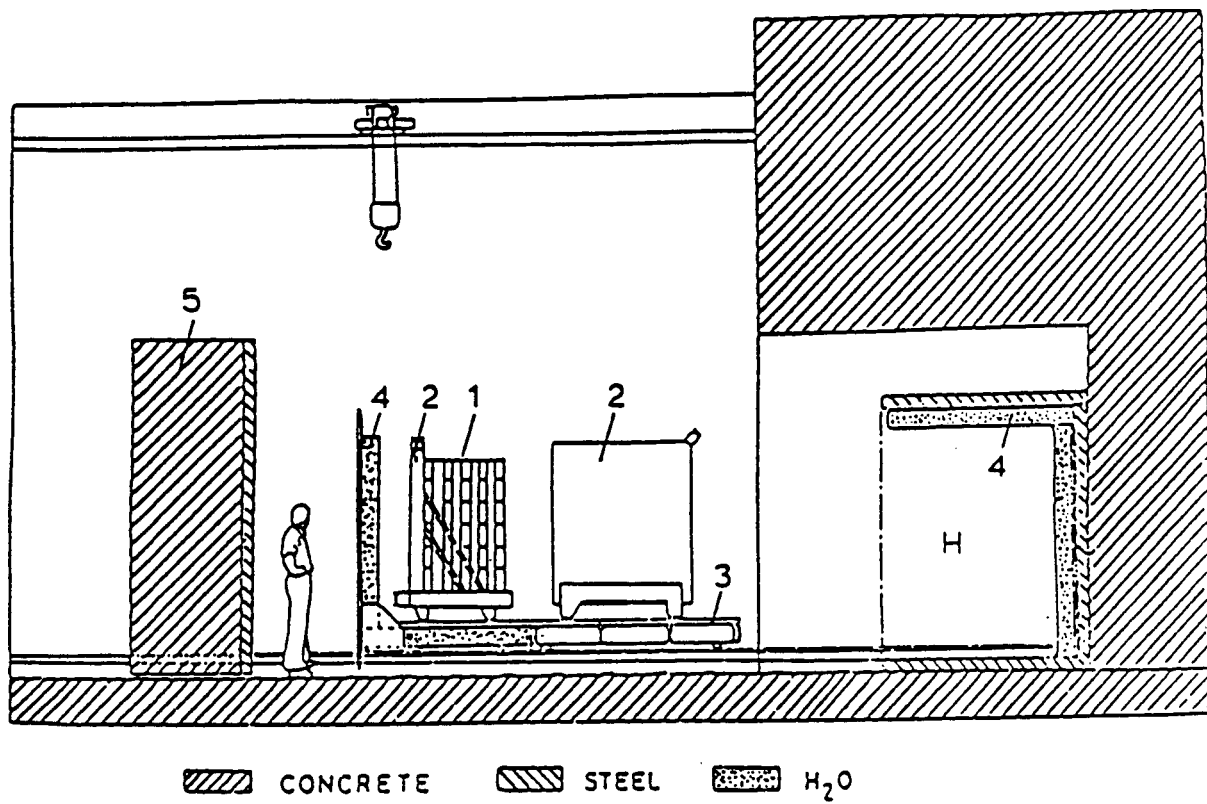


Fig. 3

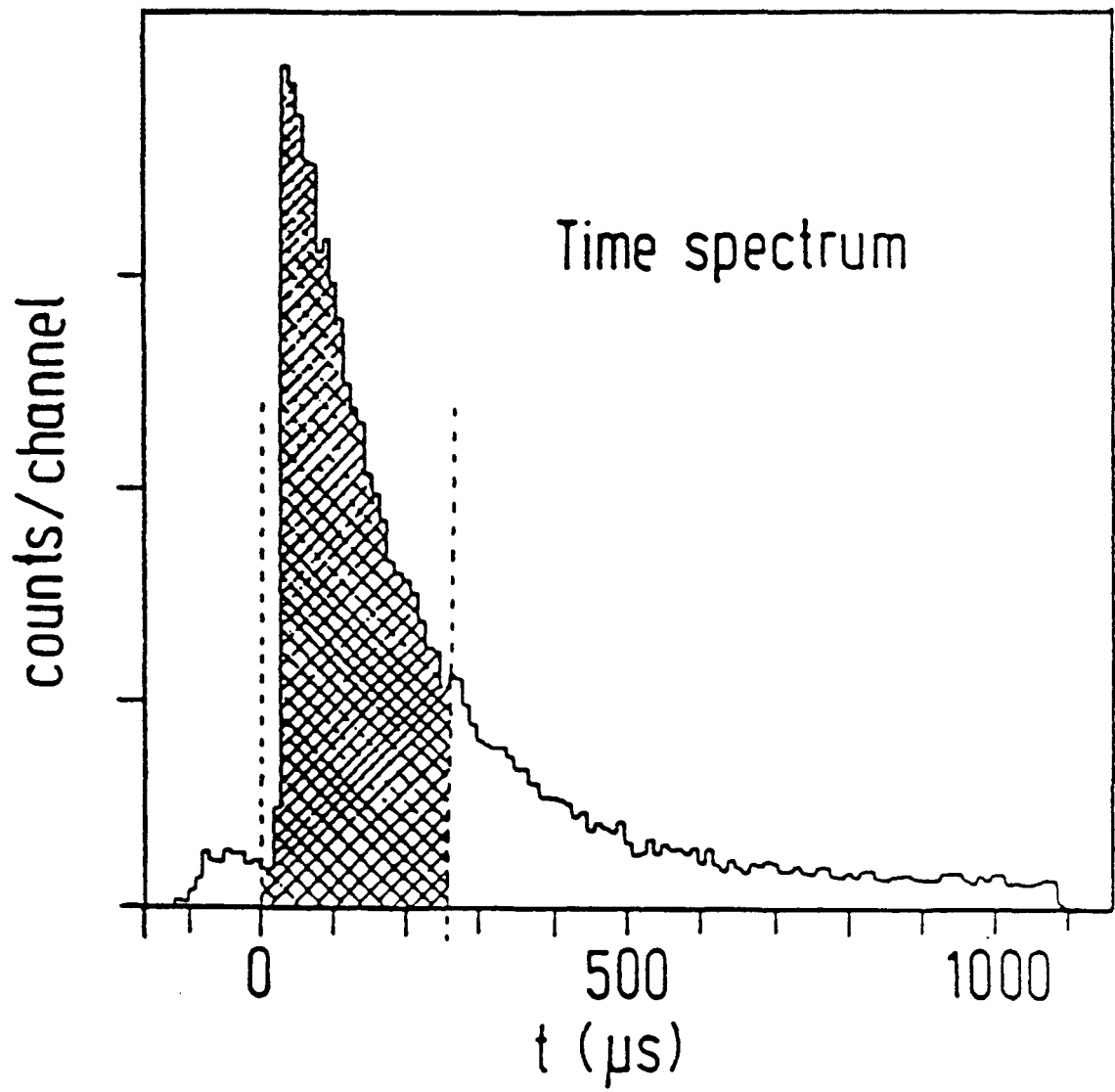


Fig. 4

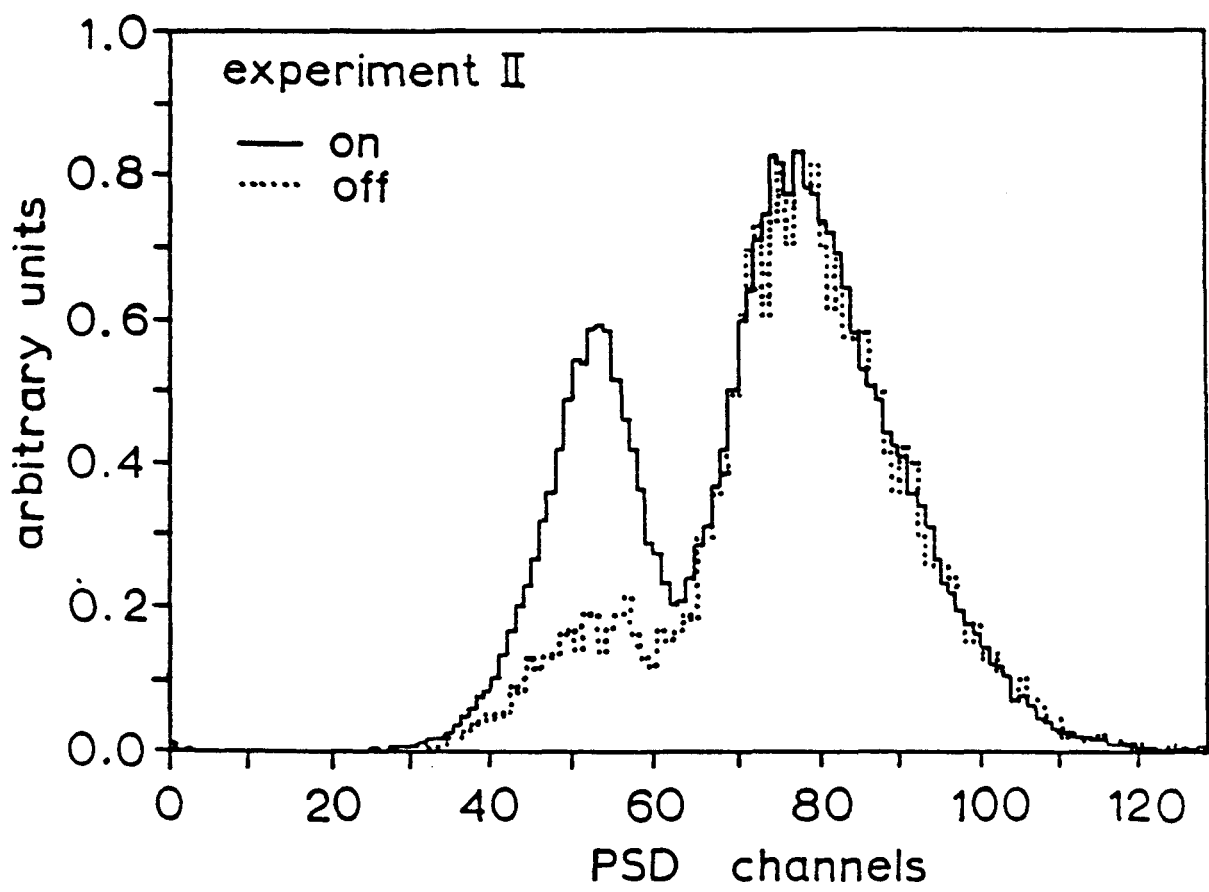


Fig. 5

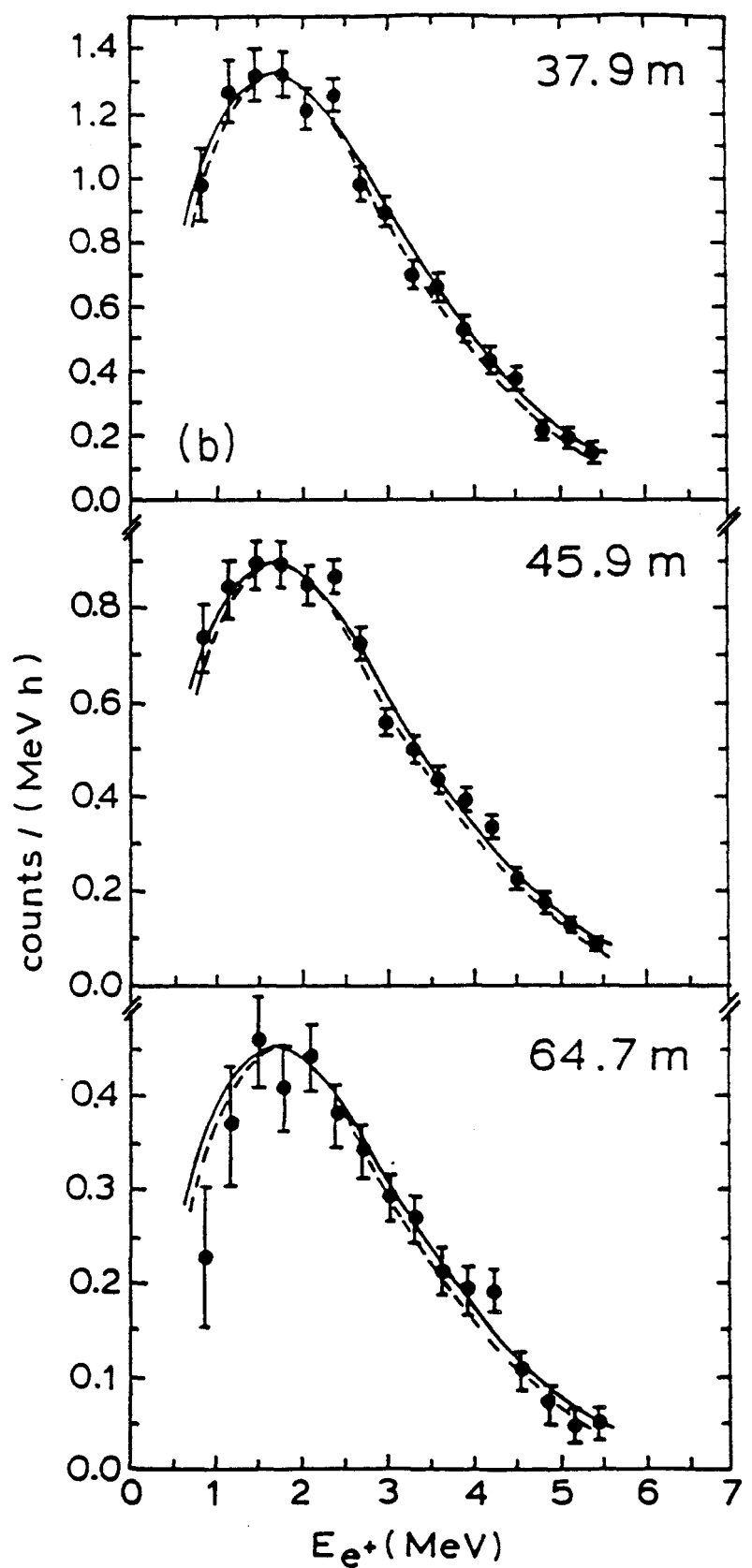


Fig. 6

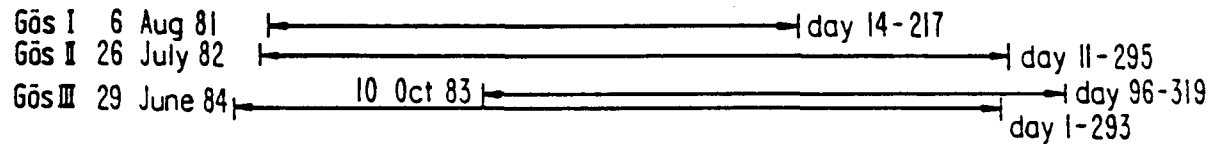
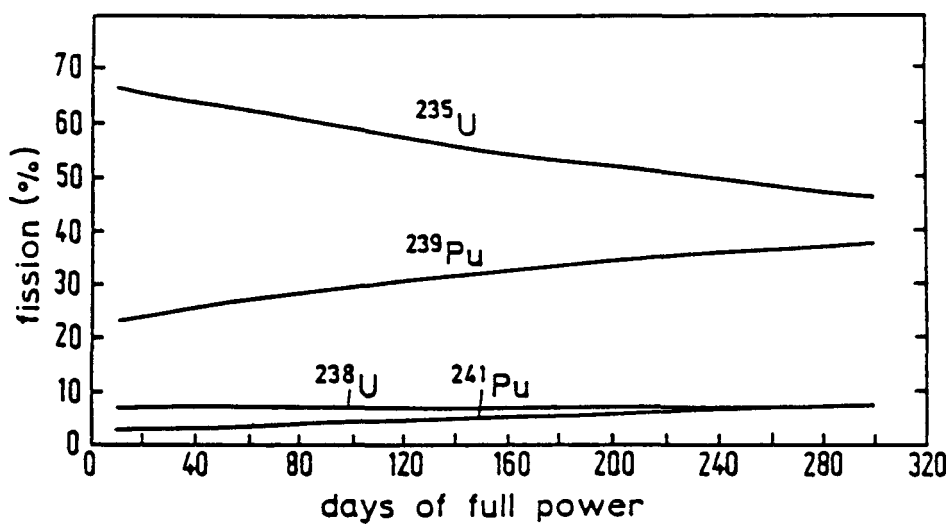


Fig. 7

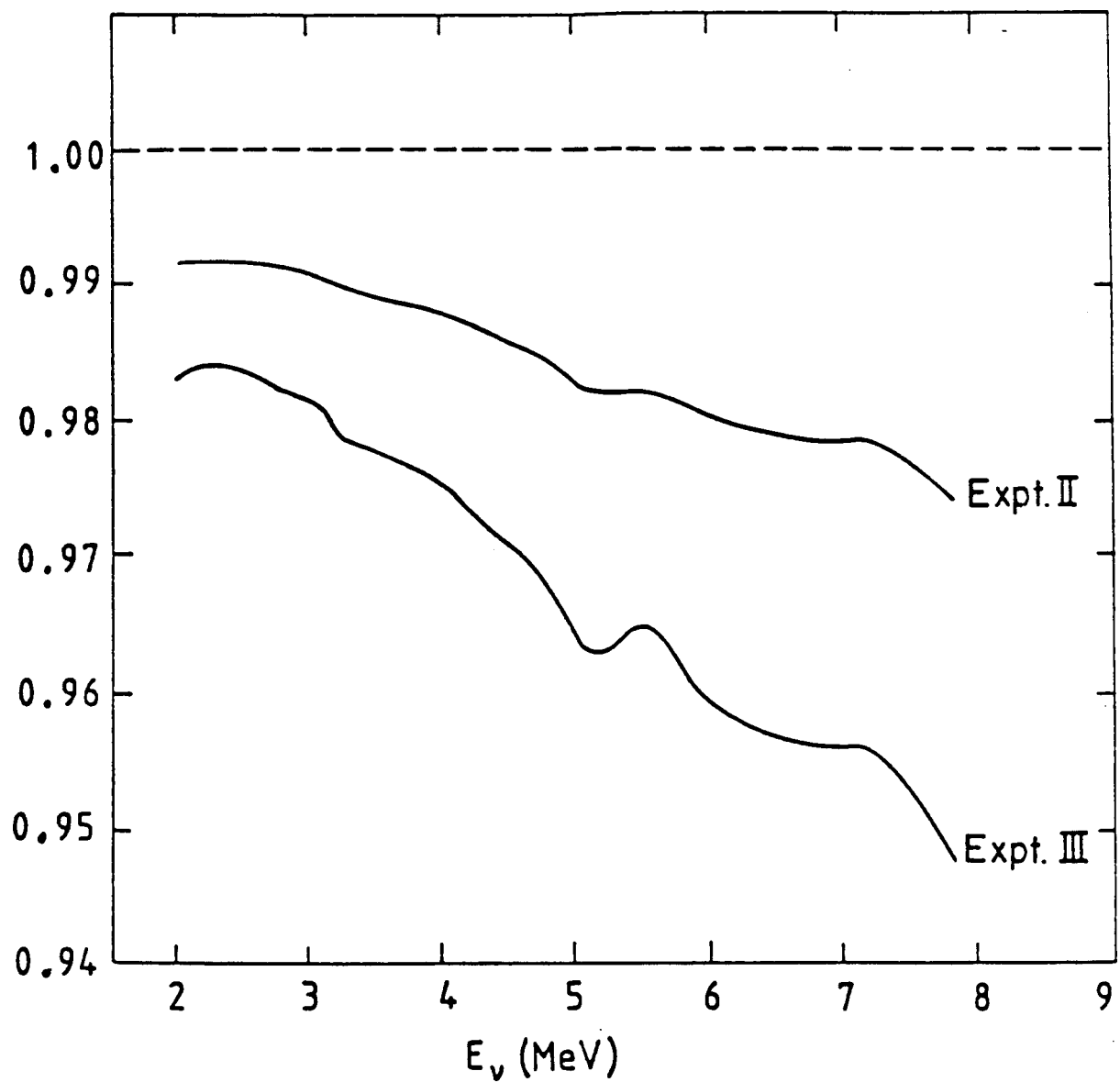


Fig. 8

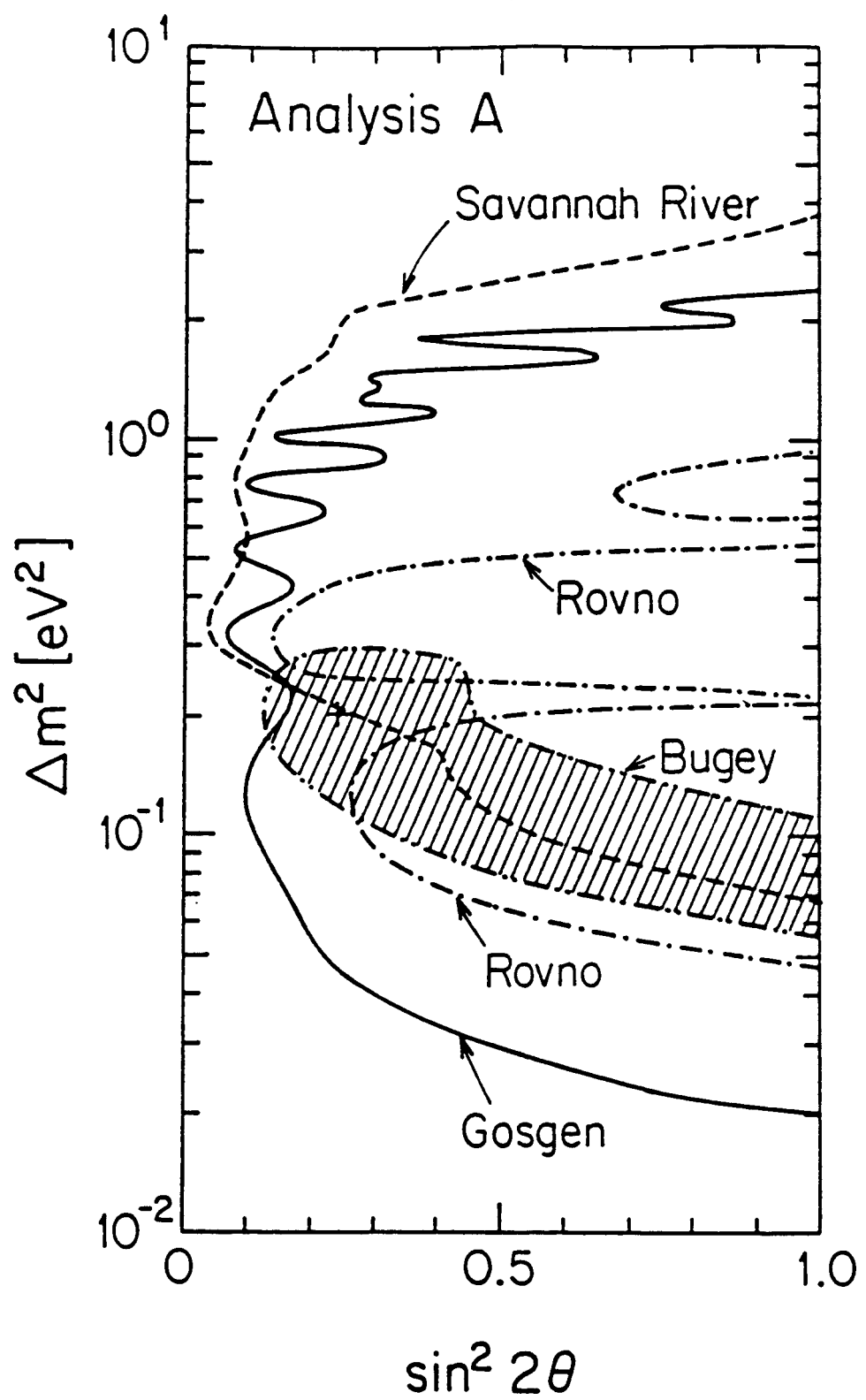


Fig. 9

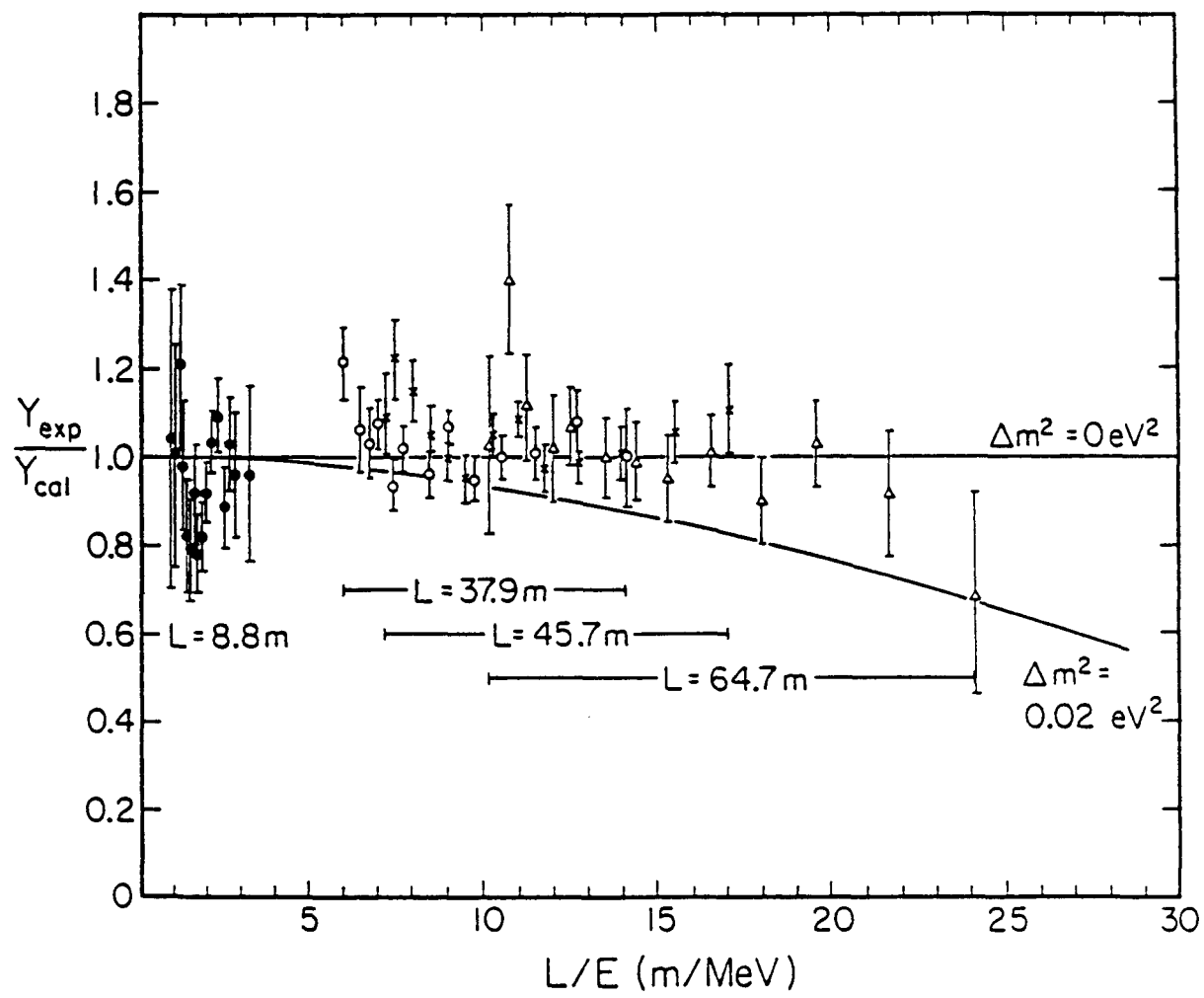


Fig. 10

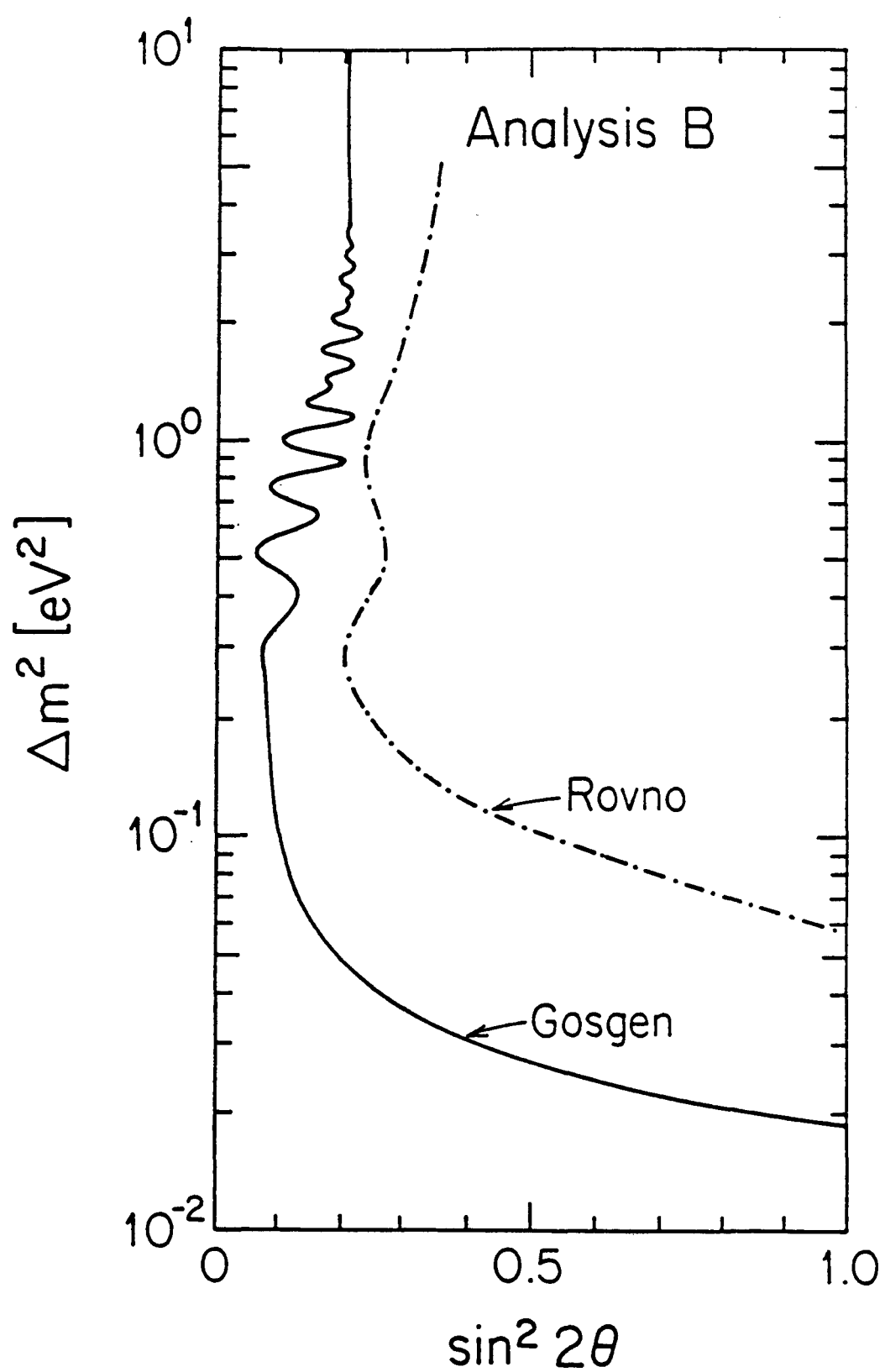


Fig. 11

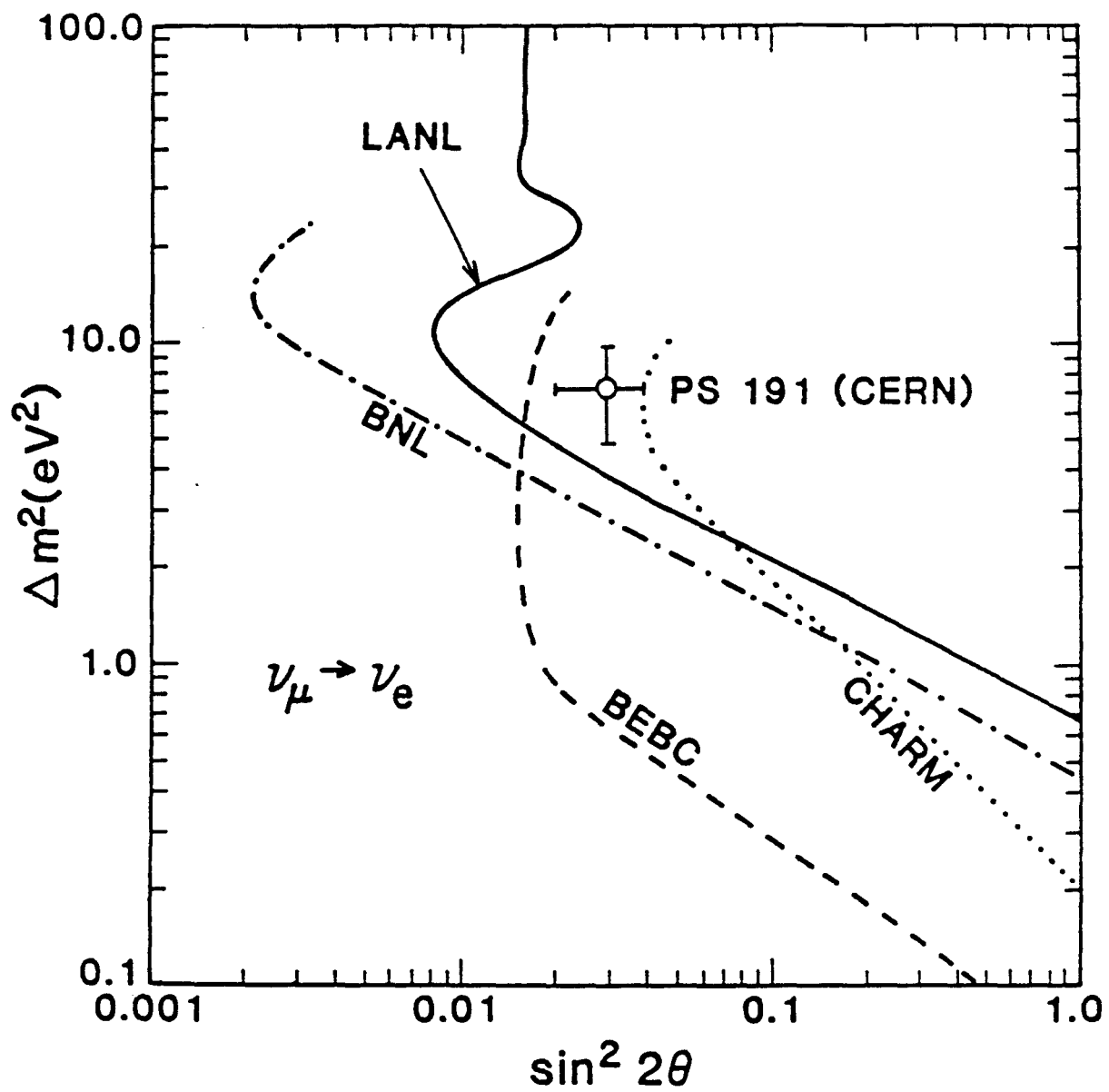


Fig. 12

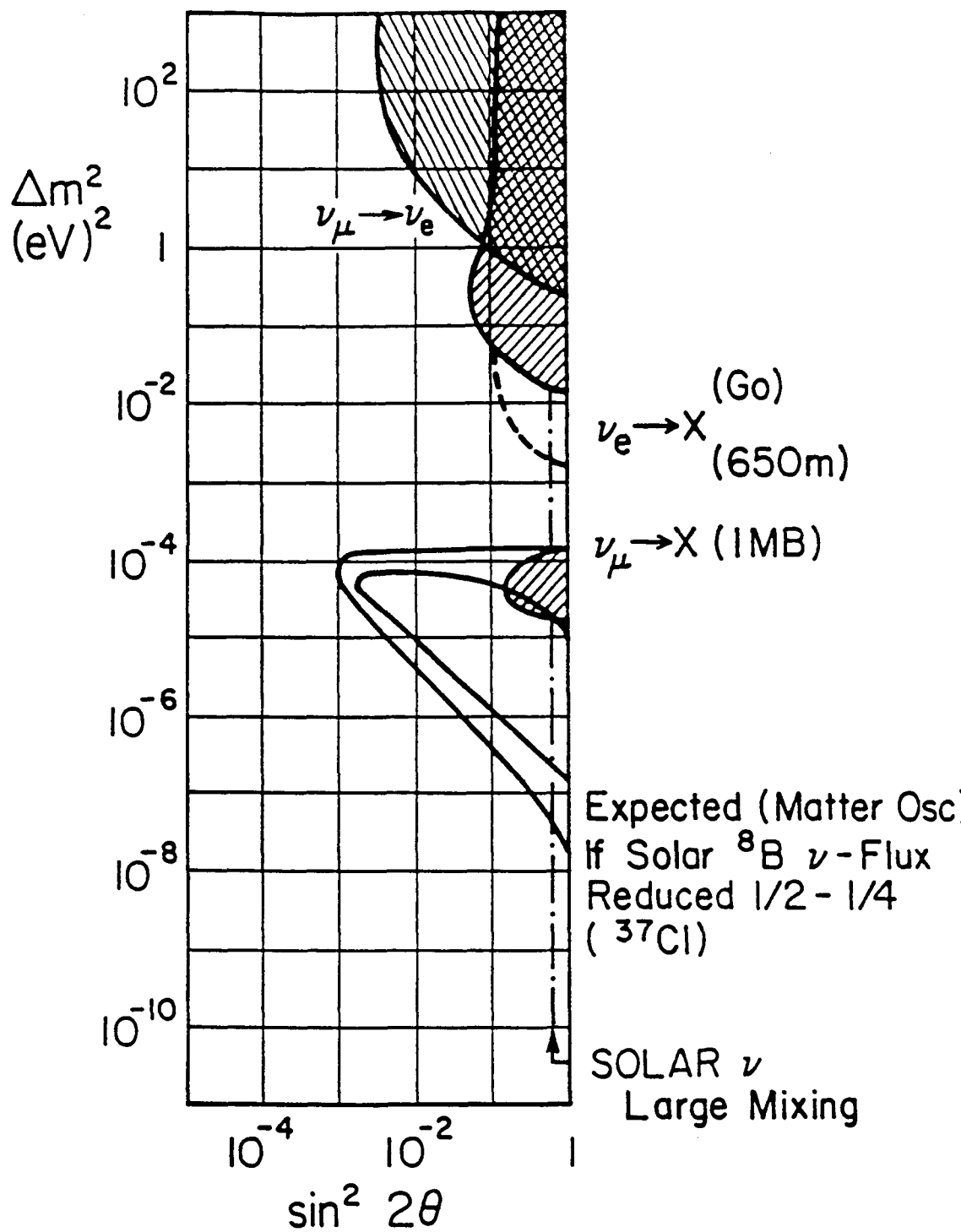


Fig. 13

TABLE I: REACTOR EXPERIMENTS

Reactor(MW)	Detector	L	#.Counts
ILL(57) <i>Caltech ISN Grenoble TU Munich</i>	377 l Liq.Sc. + ^3He $\epsilon = 0.20, 0.17$	8.8 m	0.5×10^4
Gösgen(2800) <i>Caltech SIN TU Munich</i>	$\Delta t = 250 \mu\text{s}$ $0.8 < E_{e^+} < 5.6 \text{ MeV}$	37.8 m 45.9 m 64.7 m	1.1×10^4 1.1×10^4 0.9×10^4
Bugey(2800) <i>ISN Grenoble Annecy</i>	321 l Liq.Sc. + ^3He $\epsilon = 0.26$ $\Delta t = 200 \mu\text{s}$ $1.5 < E_{e^+} < 6.5 \text{ MeV}$	13.6 m 18.3 m	4.0×10^4 2.3×10^4
Savannah River(2300) <i>Irvine</i>	300 l Liq.Sc. + Gd $\epsilon \approx 0.5$ $\Delta t = 15 \mu\text{s}$ $1.0 < E_{e^+} < 9 \text{ MeV}$	18.2 m 23.7 m	3.8×10^4 1.9×10^4
Rovno(1400) <i>Moscow</i>	240 l Liq.Sc. + Gd 136 kg Polyeth. + ^3He $\epsilon = 0.29, 0.52$	18.5 m 25.0 m	

References: ILL Ref. 2, Gosgen Ref. 3-11, Bugey Ref. 4,
Savannah River Ref. 5, Rovno Ref. 6.

TABLE II: RESULTS FROM REACTOR EXPERIMENTS
 Ratios of Integral Yields

	Expt./Calc.	Expt(2)/Expt(1)	Evidence for Osc.
ILL	0.955 ± 0.110		No
Gö 1	1.018 ± 0.065	$(2)/(1) = 1.027 \pm 0.034$	No
2	1.047 ± 0.065	$(3)/(1) = 0.958 \pm 0.053$	No
3	0.975 ± 0.076		
Bu 1	≈ 1.0	0.907 ± 0.025	Yes
2	≈ 0.9		
SR 1		$0.963 \pm (0.013 \text{st.})$	No
2			
Rov 1	0.997 ± 0.06	$0.986 \pm 0.037 \pm 0.029$	No
2			